Soft Matter

Cite this: *Soft Matter*, 2012, **8**, 7638

www.rsc.org/softmatter

PAPER

Injectable *in situ*-forming hydrogels for a suppression of drug burst from drug-loaded microcapsules

Da Yeon Kim,[a] Doo Yeon Kwon,[a] Bit Na Lee,[a] Hyo Won Seo,[a] Jin Seon Kwon,[a] Bong Lee,[b] Dong Keun Han,[c] Jae Ho Kim,[a] Byoung Hyun Min,[a] Kinam Park[d] and Moon Suk Kim*[a]

Received 12th March 2012, Accepted 23rd May 2012
DOI: 10.1039/c2sm25566a

Here, we describe the preparation of microcapsule formulations using *in situ*-forming hydrogels to achieve desired therapeutic levels over a specific period. Bovine serum albumin (BSA)-fluorescein isothiocyanate (FITC)-loaded microcapsules were prepared using a mono-axial nozzle ultrasonic atomizer with an encapsulation efficiency of approximately 65% and a particle size of approximately 60 μm. Injectable formulations were prepared by mixing BSA-FITC-loaded microcapsules (Cap) and chitosan (CH), Pluronic (PL), or methoxy poly(ethylene glycol)-*b*-poly(ε-caprolactone) (MPEG-*b*-PCL) solution (MP). All formulations were prepared as solutions and became gelatinous drug depot implants after injection into the subcutaneous tissue of Sprague-Dawley (SD) rats. While monitoring *in vivo* BSA release, we found that the initial burst release of BSA was retarded by *in situ*-forming hydrogels. The T_{max} and C_{max} values for each formulation were significantly higher and lower, respectively, than those of the BSA-FITC-solution alone. The absolute bioavailability of BSA-FITC from each formulation depended on the viscosities of the *in situ*-forming hydrogels. The viscosities of the *in situ*-forming hydrogels were considered to be an important factor influencing the initial burst and duration of BSA release over a period of several weeks. One conclusion that might be drawn from this work is that the initial burst and sustained entire release profile depend on the hydrogel properties. In conclusion, we believe the results of the present study provide potential new insights into sustained pharmacological performance and represent a useful experimental platform using *in situ*-forming hydrogels for future protein delivery research.

Introduction

Protein delivery systems have been widely investigated for their ability to improve the bioavailability of proteins and protect them from degradation in the body.[1,2] Considerable efforts have been devoted to the control and maintenance of the long-term *in vivo* release of proteins.[3] Several protein administration routes have been exploited in order to achieve this goal. Among these administration routes, microcapsules have been used to improve bioavailability and control the release of proteins over a period of several days to several weeks.[4]

In previous studies, our group manufactured protein-loaded microcapsules using a mono-axial nozzle ultrasonic atomizer (Fig. 1A).[5,6] The proteins were encapsulated in the inner core of the capsule, surrounded by a poly(D,L-lactic-*co*-glycolic acid) (PLGA) shell. The advantages of this mono-axial nozzle ultrasonic approach include a simple preparation process and less stress on the encapsulated proteins. In addition, protein-loaded microcapsules maintained *in vivo* protein release for at least 4 weeks in rats. However, these microcapsules still suffer from a major technical problem: the rapid release of protein during the first day. This initial burst was strongly believed to be the result of rapid release of proteins from the shell layer molecularly dispersed throughout the microcapsule and/or the protein released from cracked microcapsules or through microcapsule pores that rapidly perfuse through the releasing buffer under biological conditions.[7,8] After the initial burst period, the microcapsules generally have a slow release period, usually lasting for 4 weeks.

Hence, suppression of the initial burst release of proteins from microcapsules is a focus of research investigating the development of optimal protein delivery systems and includes attempts to decrease the initial burst and maintain an optimal therapeutic level of release over several periods.[3,9] One such strategy to address this problem has been to wrap the microcapsule with other matrix formulations. A different outer shell

[a]*Department of Molecular Science and Technology, Ajou University, Suwon 443-759, Korea. E-mail: moonskim@ajou.ac.kr; Fax: +82-31-219-3931; Tel: +82-31-219-2608*
[b]*Department of Polymer Engineering, Pukyong National University, Busan, 608-739, Korea*
[c]*Center for Biomaterials, Korea Institute of Science and Technology, Seoul 136-791, Korea*
[d]*Departments of Biomedical Engineering and Pharmaceutics, Purdue University, IN 47907-1791, USA*

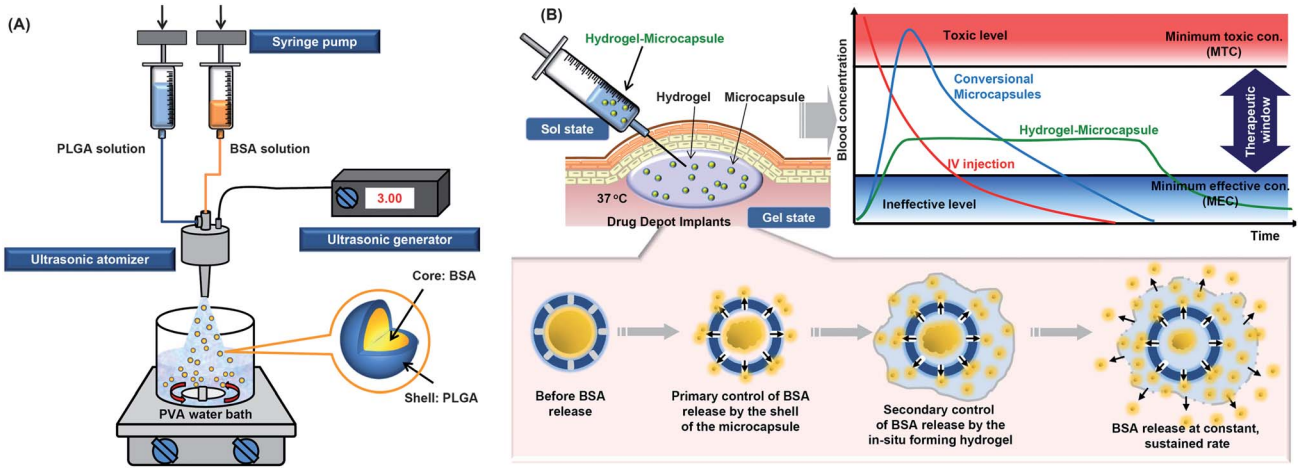

Fig. 1 Schematic representation of (A) the microencapsulation method using a mono-axial ultrasonic atomizer and (B) controlled BSA release from drug depot implants.

may induce the retardation of proteins released from the microcapsule.

The use of *in situ*-forming hydrogel is based on the idea that biomaterials that undergo a simple liquid-to-gel phase transition under physiological conditions can be injected as a liquid and can then form an *in situ* hydrogel that acts as a drug depot.[10–12] Meanwhile many researchers have proposed that *in situ*-forming hydrogels form spontaneously or in response to certain biological triggers.[13] The most interesting stimulus is temperature, which can trigger responses that fall into two main categories: electrostatic (ionic) and hydrophobic interactions.

Chitosan with primary ammonium cations is a typical *in situ*-forming hydrogel that functions *via* electrostatic (ionic) interactions with anionic compounds, such as anionic glycerol phosphate disodium salt (GP).[14] Poly(ethylene oxide) (PEO) and poly(propylene oxide) (PPO) block copolymers are the most widely used *in situ*-forming hydrogels, commercially available in solutions known as Pluronics.[15–17] Pluronic solutions undergo gelation mediated by hydrophobic interactions among poly(propylene glycol) (PPG) segments. Recently, our group reported that aqueous solutions of methoxy poly(ethylene glycol)-*b*-poly(ε-caprolactone) (MPEG-*b*-PCL) diblock copolymers served as *in situ*-forming hydrogels due to the ability of PCL hydrophobic segments to aggregate.[18–22] Chitosan (CH), Pluronic (PL), and MPEG-*b*-PCL (MP) gels can act as *in situ*-forming hydrogels and have different hydrogel properties, such as mechanical gel strength, gel persistence times, and immunoreactivity.

Because these *in situ*-forming hydrogel systems are liquid at room temperature, protein-loaded microcapsules can be mixed simply by using the components. A combination of *in situ*-forming hydrogel and protein-loaded microcapsules can make effective injectable formulations. Injectable formulations of *in situ*-forming hydrogels and protein-loaded microcapsules can then be introduced into the body at the target location in a minimally invasive manner prior to solidification or gelation.

We therefore hypothesized that *in situ*-forming hydrogel systems, acting as an additional outer shell for protein-loaded

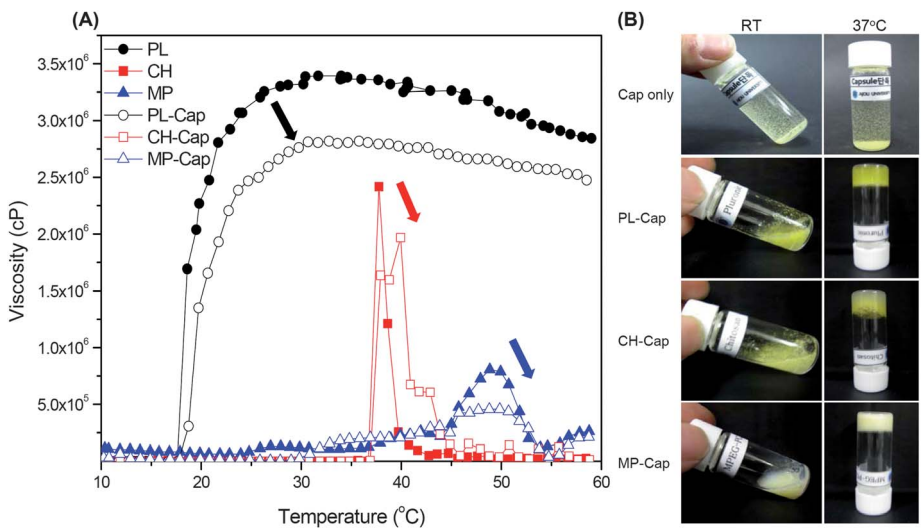

Fig. 2 (A) Viscosity *versus* temperature curves for PL, PL-Cap, CH, CH-Cap, MP, and MP-Cap solutions and (B) the images of each formulation.

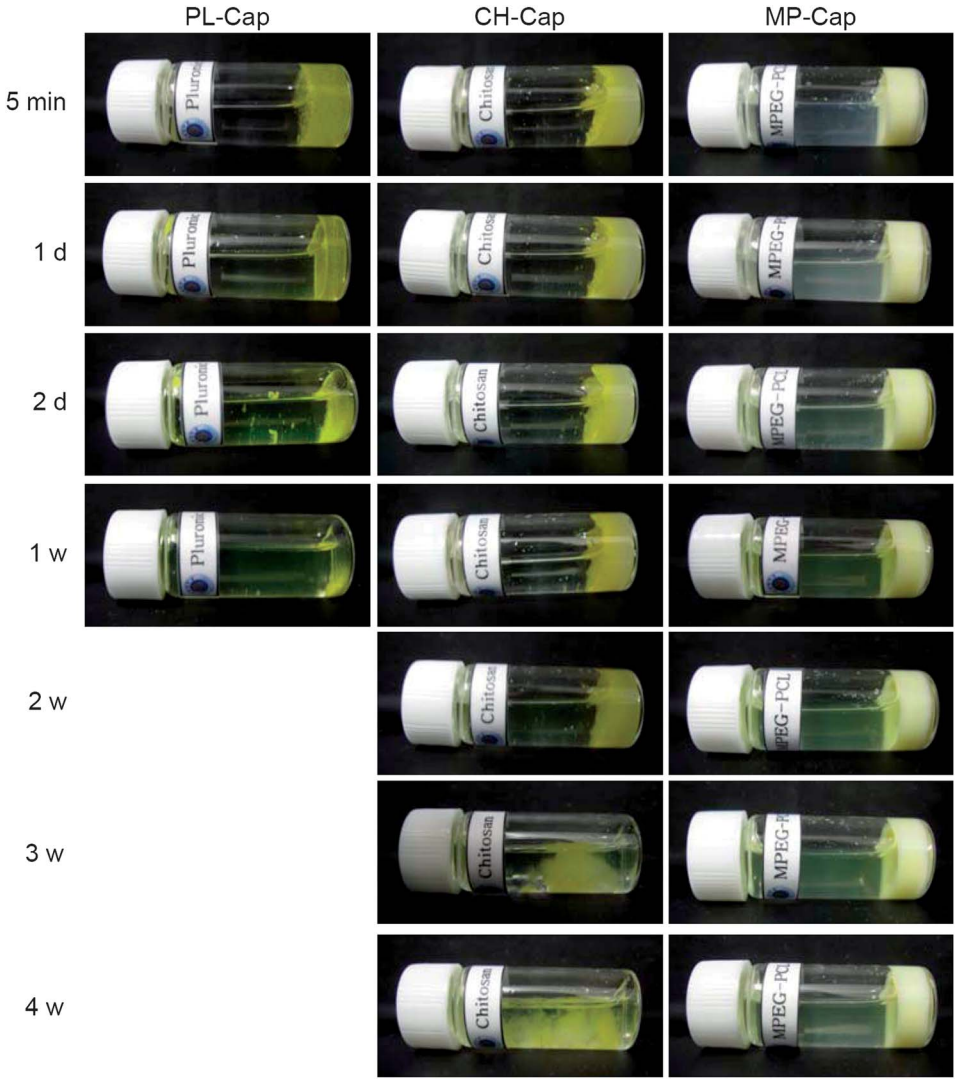

Fig. 3 Images of PL-Cap, CH-Cap, and MP-Cap after 5 min to 4 weeks at 37 °C.

microcapsules, can retard the initial burst of proteins released from microcapsules (Fig. 1B). This may be the easiest method through which to suppress the initial burst release. Therefore, the objectives of the current study were to evaluate the following questions: (1) can injectable formulations of *in situ*-forming hydrogel systems and protein-loaded microcapsules be introduced into the body to produce drug depots in a minimally invasive manner? (2) Can injectable formulations of *in situ*-forming hydrogel systems and microcapsules suppress the initial burst release of proteins from microcapsules and maintain an optimal therapeutic drug level over the desired period? (3) What hydrogel properties affect the control of protein release from microcapsules?

Experimental section

Materials

Low molecular weight PLGA (lactic–glycolic acid: 50/50, M_w: 33 000 Da) was purchased from Birmingham Polymers, Inc. (Birmingham, AL). Poly(vinyl alcohol) (PVA, 87–89% hydrolyzed, M_w: 85 000–124 000 Da) purchased from Sigma (Milwaukee, WI) was used as an emulsifier. Fluorescein isothiocyanate (FITC)-labeled bovine serum albumin (BSA) was purchased from Sigma (St. Louis, MO). Pluronic F-127 was used as received from BASF. Chitosan (medium molecular weight, 75–85% deacetylated) was purchased from Sigma–Aldrich (MI, USA). All other chemicals were analytical grades and used without further purification.

Micro-encapsulation of BSA-FITC using a mono-axial nozzle ultrasonic atomizer

Microcapsules were generated using a mono-axial nozzle ultrasonic atomizer (Sono-Tek Corp, Milton, NY). The typical preparation was achieved as follows: a PLGA solution in ethyl acetate and an aqueous solution containing BSA-FITC were separately fed into an ultrasonic atomizer. The flow rates of the PLGA solution and BSA-FITC aqueous solution were 4 and 0.2 mL min^{-1}, respectively. The concentrations of PLGA and BSA-FITC were 3% and 5% w/v, respectively. Microdroplets

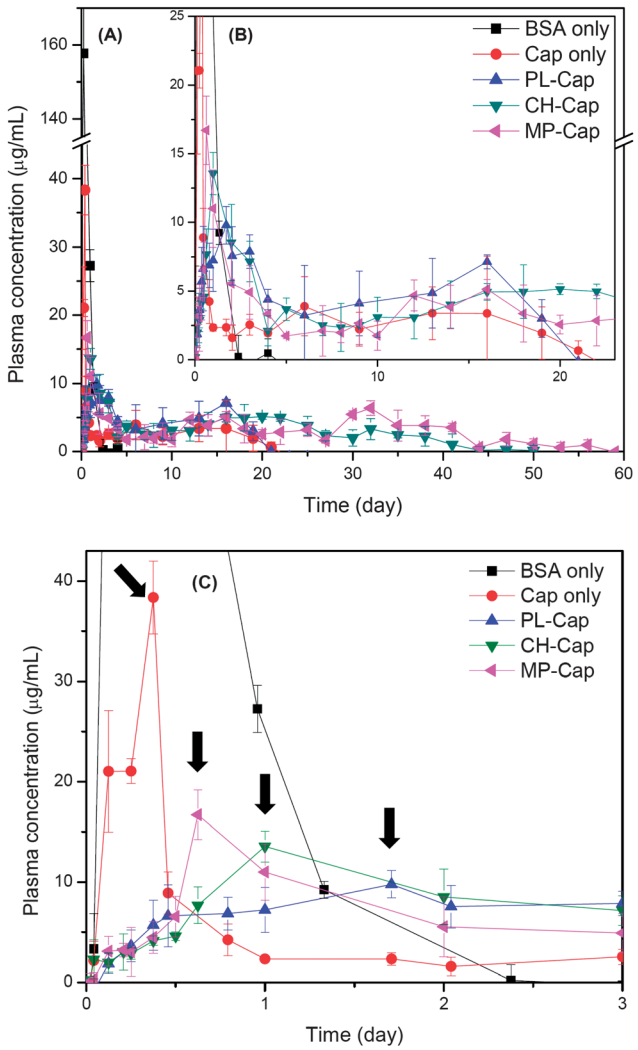

Fig. 4 Time course of BSA-FITC concentration in plasma over (A) 60 days, enlarged graph for (B) 23 days, and (C) 5 days after injection of hydrogel-BSA-FITC-loaded microcapsules. The arrows indicate the T_{max} of each formulation.

were produced by atomizing of the mixed solutions of PLGA and BSA-FITC for approximately 5 s at a vibration frequency of 3 W/60 kHz, and they were then immediately collected in a 0.5% w/v PVA solution for 2 min. The distance between the atomizer head and aqueous PVA solution was 1 cm, and the stirring speed of the PVA solution was 1000 rpm. Resulting solutions were gently stirred for 2 h to allow solidification of microcapsules, and were then washed with distilled water. The solution was frozen at −74 °C, followed by freeze-drying for 4 days. The morphology of the obtained microcapsules was observed using an optical microscope (Carl Zeiss Microimaging GmbH, Göttingen, Germany).

Encapsulation efficiency of BSA-FITC-loaded microcapsules

The encapsulation efficiency of BSA-FITC was determined using CH_2Cl_2 and distilled water (DW). Microcapsules (10 mg) were placed into a test tube and 0.4 mL CH_2Cl_2 was added to dissolve the polymer portion of the microcapsules. Then, 1.8 mL DW was added to allow solubilization of the BSA-FITC. The resulting mixture was sonicated for 90 min at 25 °C and centrifuged at 10 000 rpm for 5 min. The amount of BSA-FITC was analyzed using fluorescence spectroscopy (F-6500, Jasco, Tokyo, Japan) with an excitation wavelength of 490 nm (bandwidth 3 nm), emission wavelength of 525 nm (bandwidth 3 nm), and response time of 2 s. The encapsulation efficiency (E) was defined as follows:

$$E = [(\text{amount of encapsulated BSA-FITC})/(\text{total amount of BSA-FITC added})] \times 100.$$

Preparation of an *in situ*-forming hydrogel solution

For preparation of the CH solution, 400 mg of CH was dissolved in 18 mL of 0.1 M acetic acid prepared in DW. To produce the *in situ*-forming CH solution, 1 mL of GP solution (150 mg mL^{-1}) was added dropwise to 4 mL of CH, to yield a 30% w/w GP. The obtained liquid solution was translucent and homogeneous. For the MP diblock copolymer solution, the MP diblock copolymer (750–2400 Da) was prepared using a block copolymerization method reported previously.[15–18] MP diblock copolymers were dissolved in deionized water at 20% w/v in 4 mL vials at 80 °C and then stored at 4 °C for 48 h. For the PL solution, the PL polymer was dissolved in deionized water at 20% w/v in 4 mL vials at 0 °C and then stored at 4 °C for 48 h.

Viscosity measurements

Viscosity was measured using a Brookfield Viscometer DV-III Ultra with a programmable rheometer and circulating bath with a programmable controller (TC-502P). The viscosity measurement in the vessel was performed using a tight cap to prevent the

Table 1 T_{max}, C_{max}, and bioavailabilities of each formulation and BSA-FITC solution alone[a,b]

Formulation	T_{max}	C_{max}	AUC_0 (μg mL^{-1} day)	Relative bioavailability[c] (%)
BSA solution	6	157.9 ± 33.8	83.1 ± 11.8	100
Cap only	9	38.6 ± 3.6	55.9 ± 5.2	78.8 ± 20[d]
PL-Cap	41	9.8 ± 1.4	94.6 ± 18.9	113.8 ± 22.8
CH-Cap	24	13.6 ± 1.5	153.6 ± 7.1	184.7 ± 8.5[d]
MP-Cap	15	16.7 ± 2.5	176.7 ± 19.7	212.6 ± 23.9[d]

[a] Values are the mean ± SD ($n = 3$). [b] Evaluation times were 60 days for Cap only, PL-Cap, CH-Cap, and MP-Cap and 4 days for BSA-FITC solution alone. [c] Bioavailability = (AUC value for each formulation administration)/(mean AUC value for administration of BSA-FITC solution alone). [d] $P <$ 0.01 *versus* BSA-FITC solution alone.

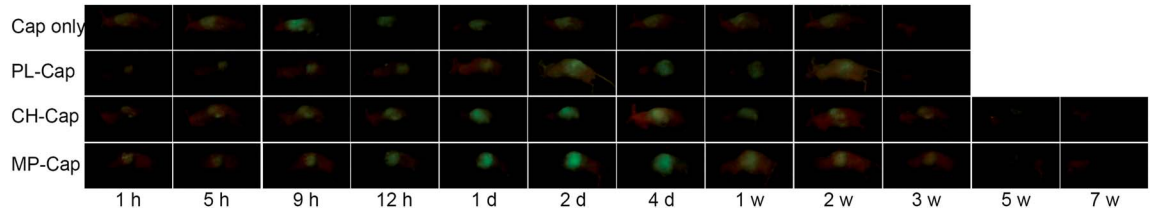

Fig. 5 *In vivo* fluorescence images of a nude mouse injected with each formulation.

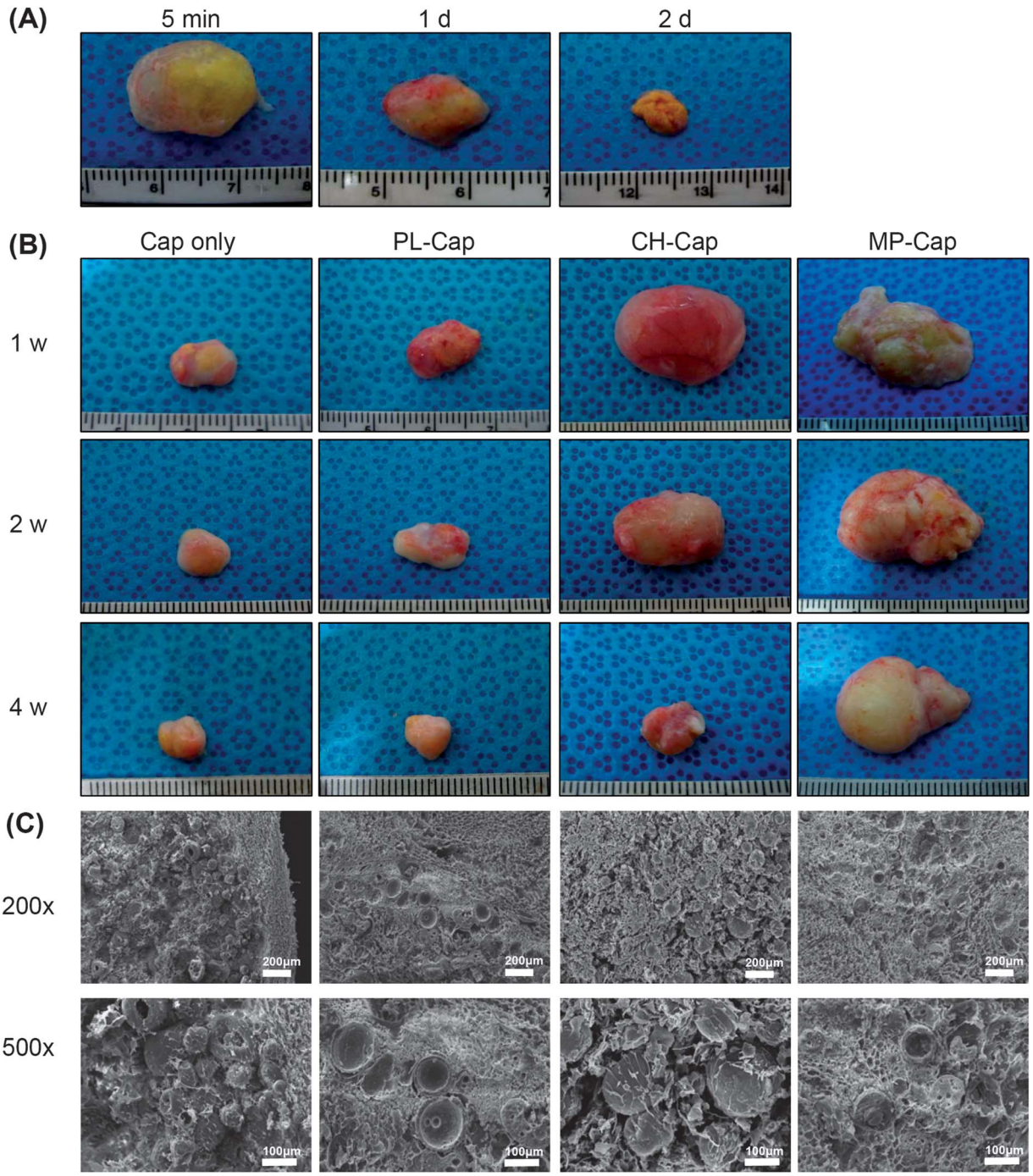

Fig. 6 (A) Optical images of excised PL-Cap at the time of sacrifice at 5 min, 1 day, and 2 days, and (B) Cap-only, PL-Cap, CH-Cap, and MP-Cap at the time of sacrifice after 1, 2, and 4 weeks. (C) SEM images of excised drug depot implants at the time of sacrifice after 1 day.

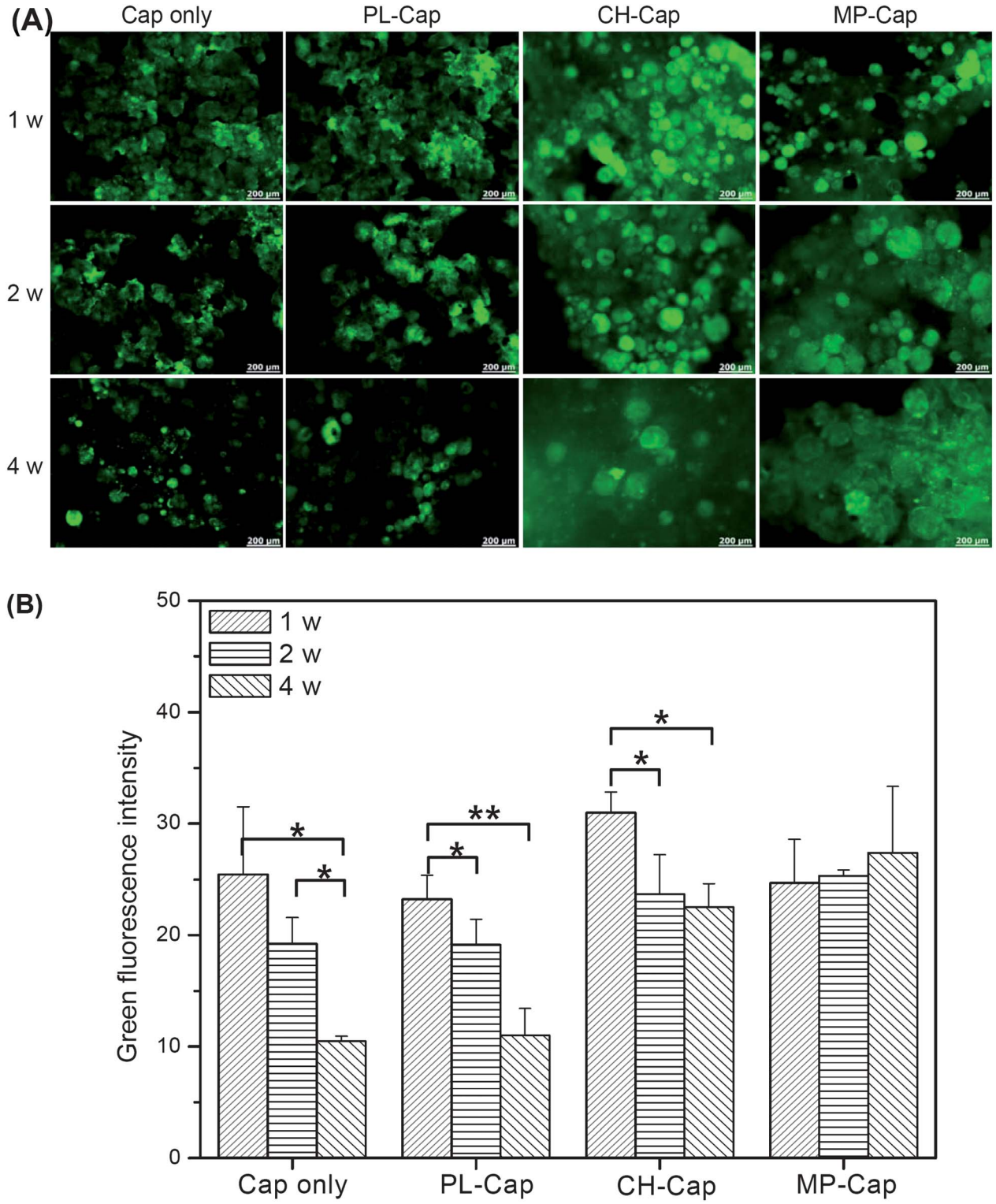

Fig. 7 (A) Fluorescence images of excised drug depot implants at the time of sacrifice after 1, 2, and 4 weeks and (B) fluorescence intensity calculated from each fluorescence image from (A). Statistical analysis was performed using one-way-ANOVA with Bonferroni's multiple comparisons (*$p < 0.05$ and **$p < 0.01$).

evaporation of water from the CH, MP, and PL solutions. The viscosities of the solutions were investigated using a T-F spindle at 0.2 rpm from 10–60 °C in 1 °C increments.

In vivo injections

CH, PL, and MP solutions were sterilized using UV light (CH solution) and ethylene oxide (EO) gas (PL and MP solutions).

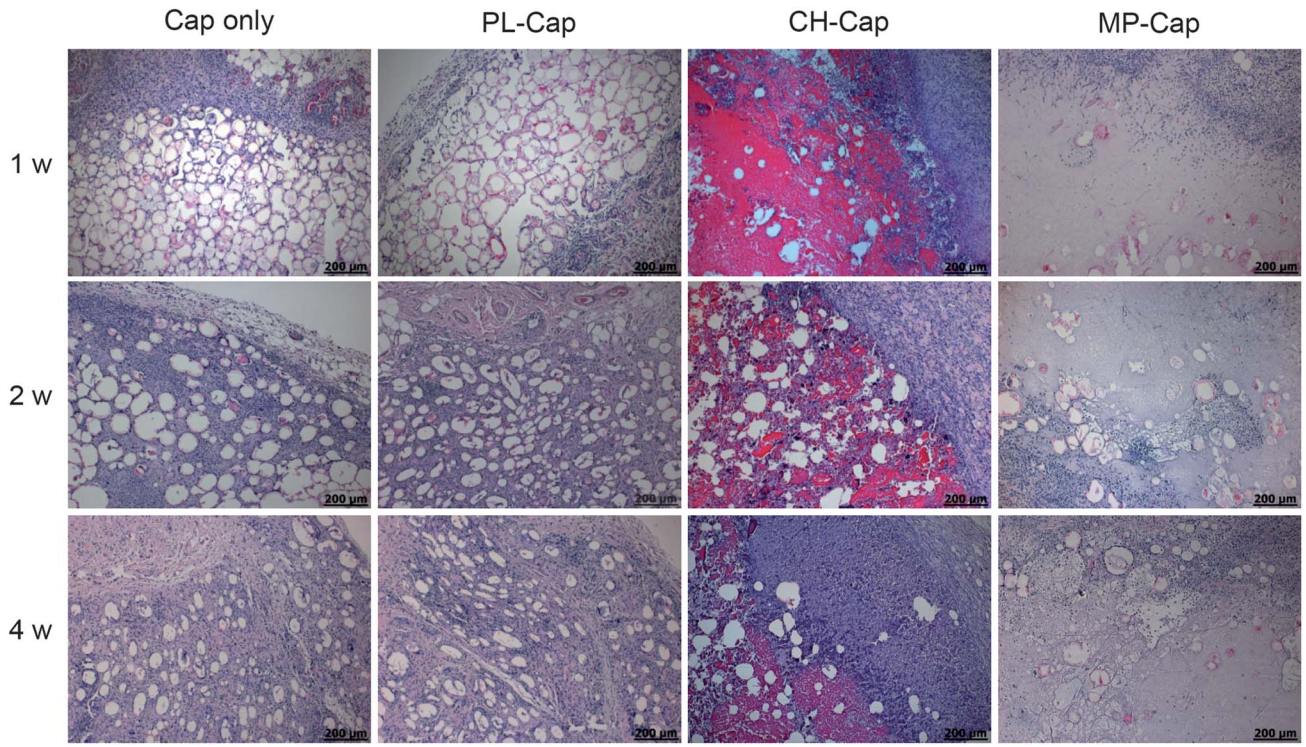

Fig. 8 H&E staining of excised drug depot implants at 1, 2, and 4 weeks after injection. Magnification is 40× for the first row and 200× for the second and third rows.

BSA-FITC-loaded microcapsules (20.1 mg) were added to 4 mL vials containing 1 mL injectable *in situ*-forming solution in each vial. For the microcapsule control sample, 1 mL of BSA-FITC-loaded microcapsules (20.1 mg) was prepared using a 20% w/v solution of 5% D-mannitol, 2% carboxymethylcellulose, and 0.1% Tween 80 as an injection vehicle. For the BSA-FITC control sample, BSA-FITC was prepared in PBS. The amount of BSA-FITC in the final solution was 2 mg mL^{-1} for all formulations. Sprague-Dawley (SD) rats (320–350 g, age 8 weeks) were used in the *in vivo* release tests. The rats were housed in sterilized cages, with sterile food and water and filtered air, and were handled in a laminar flow hood under aseptic conditions. All animal treatments and surgical procedures followed approved protocols and were performed in accordance with the Institutional Animal Experiment Committee at the Ajou University School of Medicine.

Each solution of 1 mL volume was injected using a 21-gauge needle into the subcutaneous dorsum of rats that had been anesthetized with ethyl ether and became gel of calc. 0.202 g *in vivo*. For the *in vivo* detection of BSA-FITC, an aliquot of blood was drawn from the tail vein of each rat at specified blood collection times. For the analysis of blood samples, 0.3 mL aliquots of blood from the catheterized tail vein were collected in Eppendorf tubes and mixed with 0.2 mL of a 1 : 499 mixture of heparin and saline, followed by gentle shaking. To obtain plasma, blood solutions were centrifuged at 1000 rpm for 5 min at room temperature. Next, 100 μL DW, 300 μL of 66 mM EDTA, and 400 μL of 50 mM HEPES (pH 7.4) were added to 200 μL plasma. Plasma samples were frozen and stored at −20 °C until assayed by fluorescence spectroscopy (F-6500, Jasco, Tokyo, Japan). To analyze the state of the probe and to examine the reliability of the method, we recorded spectra of BSA-FITC standard solutions of known BSA-FITC concentrations in blood and created standard calibration curves. The amount of cumulatively released BSA-FITC was calculated by comparison with these standard calibration curves. Each formulation was given to three rats, and the release experiment was separately performed on each rat. The results were averaged for each group of three rats. The area under the plasma BSA-FITC concentration *vs.* time curve was calculated as the AUC. The *in vivo* detection of BSA-FITC does not mean real bioavailability of BSA. In this work, we only deduced the bioavailability of BSA from the detected BSA-FITC. The relative bioavailability was calculated by comparing the AUC of each formulation to that of the BSA-FITC solution alone.

Real time *in vivo* fluorescence imaging

Six-week-old male nude mice were anesthetized with ethyl ether and treated with each formulation *via* subcutaneous injection into the left dorsum using a 21-gauge needle. At selected times, side-view images of each mouse were collected at a wavelength of 515 nm (excitation wavelength, 470 nm) using a fluorescence imaging system (FO ILLUM PL-800; 150 W EKE Quartz Halogen light, glass reference number: OG515 filter; Edmund Optics, NJ, USA). After digitization using a CCD, fluorescence images were visualized with Axiovision Rel. 4.8 software.

Scanning electron microscopy *in vitro* and *in vivo*

The morphology of the *in vitro* and *in vivo* microcapsules was examined by scanning electron microscopy (SEM) using

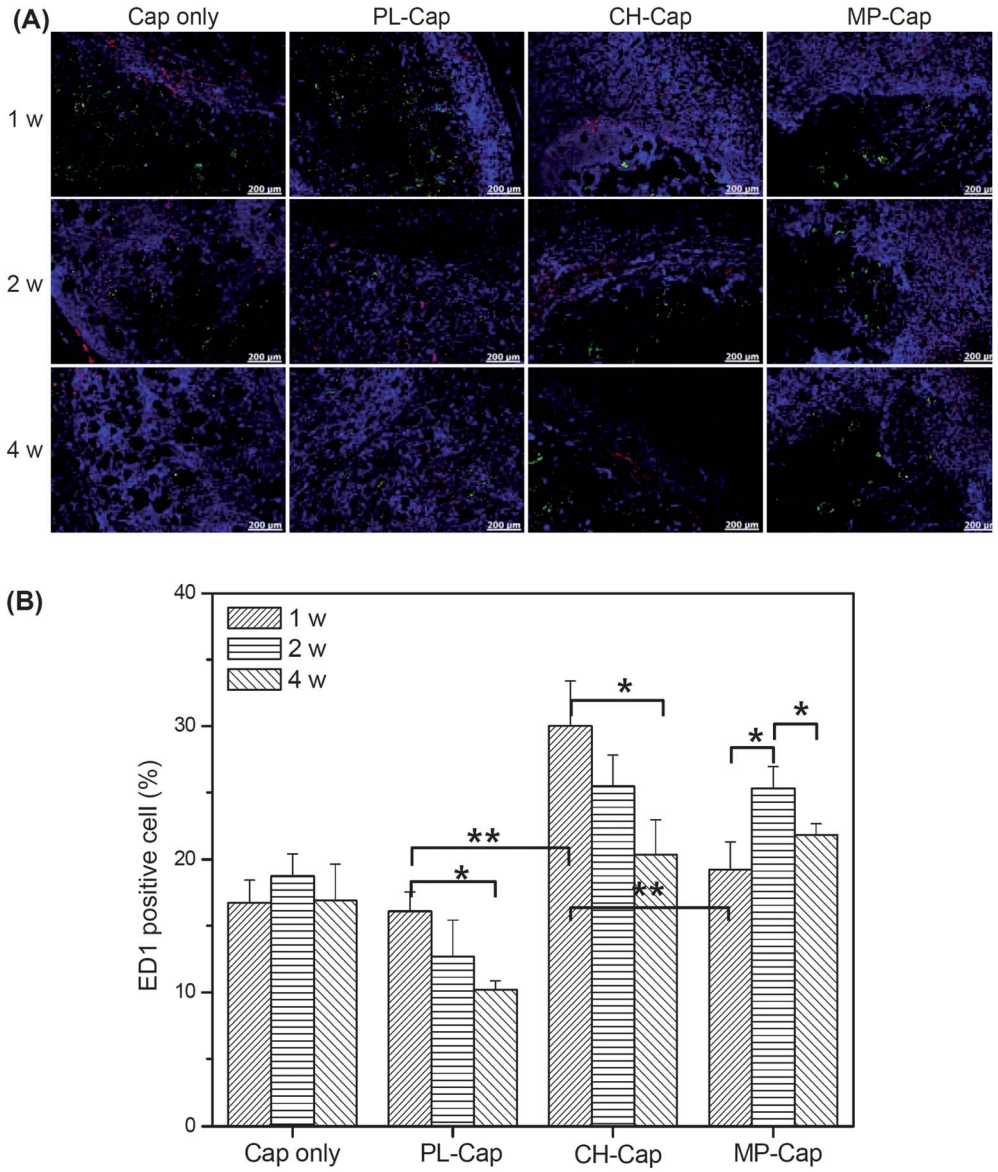

Fig. 9 (A) ED1 immunofluorescent staining of excised drug depot implants and (B) the number of ED1-positive cells on excised drug depot implants as a function of time after injection. Statistical analysis was performed using one-way-ANOVA with Bonferroni's multiple comparisons (*$p < 0.05$ and **$p < 0.01$).

a JSM-6380 SEM (JEOL, Tokyo, Japan). Immediately after being removed from the rat, the drug depot implants were mounted on a metal stub that was precooled in liquid nitrogen. After mounting the drug depot implants, the metal stub was quickly immersed in a liquid nitrogen bath to minimize alterations of the drug depot implants. The stub was then freeze-dried at −75 °C using a freeze dryer, coated with a thin layer of gold using a plasma-sputtering apparatus (Ted Pella, Cressington 108 Auto, CA, USA) under an argon atmosphere, and examined by SEM.

Fluorescence imaging of the removed depots

Drug depots were removed from SD rats at 1, 2, and 4 weeks after transplantation. Fluorescence images of implants were captured using a charge-coupled device (CCD) and visualized under an Axio Imager A1 (Carl Zeiss Microimaging GmbH, Göttingen, Germany) equipped with Axiovision Rel. 4.8 software (Carl Zeiss Microimaging GmbH). The change in fluorescence intensity was determined using Image J image processing software with standard image-editing procedures to generate a fluorescence intensity histogram of the image.

Histological analysis

At 1, 2, and 4 weeks after transplantation, the rats were sacrificed and drug depot implants were dissected individually and removed from the subcutaneous dorsum. Microcapsule-containing drug depot implants were prepared for immunohistochemical analysis by immediately fixing tissues in 10% formalin and embedding them in paraffin wax. Each embedded specimen was then sectioned (into 4 μm thick slices) along the longitudinal

axis of the drug depot implants, and the sections were stained with 4',6-diamino-2-phenylindoedihydrochloride (DAPI, Sigma, USA), ED1 (mouse anti-rat-CD68, Serotec, UK), and hematoxylin and eosin (H&E). The staining procedures for DAPI and ED1 were as follows. The slides were washed with PBS-T (0.05% Tween 20 in PBS) and were then blocked with a 5% BSA (Bovogen, Australia) and 5% HS (horse serum, GIBCO, UK) buffer in PBS for 1 h at 37 °C. Sections were incubated with mouse anti-rat-CD68 overnight at 4 °C. After washing with PBS-T, the slides were incubated with secondary antibodies (goat anti-mouse Alexa Fluor594, Invitrogen, USA) for 3 h at room temperature in the dark. After washing again with PBS-T, the slides were counter-stained with DAPI and then mounted with fluorescent mounting solution (DAKO, CA, USA). Immunofluorescence images were visualized by Axio Imager A1 and Axiovision Rel. 4.8 software, as described above.

Results and discussion

Preparation of BSA-FITC-loaded microcapsules

BSA-FITC-loaded microcapsules (Cap) were prepared using a concentric nozzle ultrasonic atomizer (Fig. 1A). Optical and SEM images demonstrated that these procedures resulted in spherical microcapsules with a smooth surface structure (data not shown). Fluorescence microscopy demonstrated the green fluorescence of the loaded BSA-FITC inside microcapsules. Cap had a mean particle size of 60 ± 12 μm. The BSA-FITC encapsulation efficiency was up to 65%. This result indicated that BSA-FITC-loaded microcapsules could be prepared with relatively high encapsulation efficiency and achieving the desired particle size through the simple process of manufacturing by using a concentric nozzle ultrasonic atomizer.

Preparation of *in situ*-forming hydrogels

Aqueous solutions of PL and MP were prepared by dissolving block copolymers in DW at 20% w/v concentration. The CH containing 30 wt% GP was also prepared in DW. PL and CH formed clear liquid solutions, but MP formed a translucent white solution. The thermosensitivity of all solutions was monitored by measuring the solution viscosity as a function of temperature from 10 to 60 °C (Fig. 2A). The viscosities of PL, CH, and MP solutions at 37 °C were 3.3×10^6, 2.4×10^6, and 0.16×10^6 cP, respectively. PL, CH, and MP exhibited sol-to-gel phase transitions at around body temperature. The strength of the respective *in situ*-forming hydrogels was PL > CH > MP at 37 °C. However, after incubation at 37 °C for 2 days, the PL gel became liquid. In contrast, CH and MP gels remained solid for 30 days at 37 °C (data not shown).

Injectable formulations were prepared by mixing Cap with each *in situ*-forming hydrogel (Fig. 2B). The PL-Cap and CH-Cap mixtures formed translucent yellow liquids due to the yellow color of FITC, while MP-Cap formed a translucent light-yellow liquid due to the original white color of MP. All formulations flowed when tilted at room temperature. At 37 °C, all formulations did not flow when tilted. All formulations exhibited distinct sol-to-gel phase transitions at 37 °C.

The viscosities of all formulations slightly decreased according to the addition of Cap. The viscosities of Cap, PL-Cap, CH-Cap, and MP-Cap solutions at 37 °C were 1, 2.7×10^6, 1.6×10^6, and 0.16×10^6 cP, respectively. The viscosity may indicate the strength of the drug depot implants formed by each formulation.

Fig. 3 shows changes in PL-Cap, CH-Cap, and MP-Cap occurring as a result of incubation at 37 °C. PL-Cap dissolved within 2 days at 37 °C, and CH-Cap maintained a gelatinous form for up to 2 weeks and then dissolved after around 3 weeks at 37 °C. However, MP-Cap maintained a gelatinous form for up to 4 weeks, indicating that drug depots arising from MP-Cap maintained their structural gelatinous integrity.

BSA-FITC release *in vivo*

To assess *in vivo* injectability and BSA-FITC release, PL-Cap, CH-Cap, and MP-Cap formulations were prepared as solutions and injected into the subcutaneous tissue of SD rats. These injectable formulations became drug depot implants in rats. For comparison, we also injected BSA-FITC solution alone and the Cap-only control. All formulations had a BSA-FITC concentration of 2 mg mL^{-1}, and *in vivo* BSA-FITC release from each formulation was monitored over time by measuring plasma BSA-FITC concentrations in rats using fluorescence spectroscopy (Fig. 4).

The T_{max}, C_{max}, and absolute bioavailability data, calculated from Fig. 4, are summarized in Table 1. The prolonged release of BSA was observed from all formulations of BSA-loaded microcapsules. However, T_{max}, C_{max}, and bioavailability values were significantly different between all formulations. T_{max} and C_{max} values for each formulation were significantly higher and lower, respectively, than those of the BSA-FITC solution alone. Injection with BSA-FITC alone revealed a C_{max} of 160 μg mL^{-1} at 6 h (T_{max}), and concentrations then rapidly declined, approaching 0 μg mL^{-1} after 2 days. Cap only showed a C_{max} of 38 μg mL^{-1} at 9 h (T_{max}) and maintained a sustained-release profile of plasma BSA-FITC concentrations for 20 days. PL-Cap had a C_{max} of 10 μg mL^{-1} at 41 h (T_{max}) and maintained a sustained-release profile for 20 days. The PL-Cap formulation exhibited high viscosity after short times at body temperature (as described in Fig. 2), but dissipation of PL was apparent after only 2 days (as described in Fig. 3 and in several previous works[23–25]). This resulted in significant suppression of the initial burst but after a short time, PL-Cap showed a similar duration of BSA release as BSA-FITC-loaded microcapsules.

CH-Cap had a C_{max} of 14 μg mL^{-1} at 24 h (T_{max}) and maintained a sustained-release profile for 45 days. The CH-Cap formulation showed medium gel strength after short times at body temperature (as described in Fig. 2), but dissolved after around 3 weeks (as described in Fig. 3). This resulted in moderate suppression of the initial burst and maintained the duration of BSA release for 45 days.

Meanwhile, plasma BSA-FITC concentrations in rats injected with MP-Cap had a C_{max} of 17 μg mL^{-1} at 15 h (T_{max}) and maintained a sustained-release profile for as long as 60 days. The MP-Cap formulation exhibited low viscosity after short times at body temperature (as described in Fig. 2) but maintained their structural gelatinous form for 4 weeks (as described in Fig. 3), resulting in low suppression of the initial burst at short times and maintaining BSA release for 60 days.

AUC_{0-t} values, calculated by measuring the area under the plasma BSA-FITC curves (AUC) from t_0 to time t using the trapezoidal rule, and absolute bioavailability of BSA-FITC were determined from the plasma concentration profiles. AUC_{0-t} values for the BSA-FITC control solution, Cap control, PL-Cap, CH-Cap, and MP-Cap were 83, 56, 95, 154, and 177 μg mL^{-1}, respectively. Absolute bioavailabilities of BSA-FITC from each formulation were approximately 78%, 114%, 185%, and 213% of the AUC_{0-t} of BSA-FITC alone. Absolute bioavailabilities of BSA-FITC from CH-Cap and MP-Cap were approximately 2–3 times higher than that of Cap only.

Increasing the viscosity decreased the initial burst, causing the lower plasma C_{max} concentrations at shorter times and extended T_{max} times in the release profile of BSA-FITC. Thus, the viscosities of the *in situ*-forming hydrogels acting as wrapping materials were considered to be important factors influencing release profiles. These results indicated that sustained release with a lower burst effect could be attributed to greater retardation of BSA diffusion.

In vivo fluorescence imaging

Fluorescent images were acquired from nude mice after subcutaneous injection of Cap only, PL-Cap, CH-Cap, and MP-Cap (Fig. 5). High levels of green fluorescence were observed at the injection site shortly after injection, and diffusion was apparent after injection. After this time, both the intensity and area of fluorescence gradually decreased. For Cap only and PL-Cap, negligible fluorescence intensities were observed after 3 weeks, and none was observed after 4 weeks. Meanwhile, fluorescent signals from CH-Cap and MP-Cap were observed even after 5 weeks, indicating the sustained release of BSA.

Morphology of the *in vivo* microcapsules

To investigate the controlled release of BSA-FITC beyond weeks, drug depot implants in tissues excised from rats after 1, 2, and 4 weeks were observed (Fig. 6). In optical images (Fig. 6A and B), the *in vivo* drug depot implants from microcapsules and hydrogels could be easily identified and isolated from the surrounding tissue. The size of the PL-Cap abruptly decreased from 5 min to 1 and 2 days, indicating the *in vivo* dissipation of PL (Fig. 6A). In terms of weeks (Fig. 6B), the sizes of Cap only, PL-Cap, and CH-Cap gradually decreased from week 1 to week 4, probably due to the *in vivo* dissipation of the hydrogel. Meanwhile, MP-Cap nearly maintained the initial size for 4 weeks, because MP increased the structural integrity of the hydrogel for long-term periods, as reported in previous work.[19] The microcapsules appeared spherical in SEM images, and the *in situ*-forming hydrogel supported the interface area of the microcapsules. The drug depot implants of PL-Cap, CH-Cap, and MP-Cap revealed that the microcapsules were interspersed in the *in situ*-forming hydrogels and interconnected hydrogel pores. The *in situ*-forming hydrogel exhibited the pore network, implying the allowance of the release of BSA.

In fluorescence images of excised drug depot implants (Fig. 7A), green fluorescence was observed, and this fluorescence represented the BSA-FITC in microcapsules or the BSA-FITC in hydrogel after releasing from microcapsules. Thus, changes in fluorescence intensity were attributed to the sustained release of BSA-FITC from each formulation. Fig. 7B shows the fluorescence intensity calculated from fluorescent images of drug depot implants. The fluorescent signal from Cap only and PL-Cap gradually decreased from 1 to 4 weeks, indicating direct release of BSA-FITC from Cap. Meanwhile, the fluorescence intensity of CH-Cap and MP-Cap was maintained for 4 weeks, indicating that BSA-FITC was maintained for extended periods in drug depot implants.

Host tissue response

To assess the local biocompatibility of each formulation, the tissues into which each drug depot implant had been transplanted were examined. H&E-stained histological sections of harvested implants revealed tissue integrity after 1, 2, and 4 weeks (Fig. 8). The Cap-only control and PL-Cap exhibited large microcapsules because the PL gel in PL-Cap disappeared within 2 days. CH-Cap-injected tissues contained a medium number of microcapsules, while MP-Cap-injected tissues contained few microcapsules, even after 4 weeks. The number of macrophages and neutrophils had increased in the border zone and near the microcapsules and *in situ*-forming hydrogels, as well as inside the tissue layer.

Response to the ED1 antibody is considered a unique *in vivo* indicator of the inflammatory response since ED1 is a macrophage marker. Therefore, tissues were stained with ED1 and DAPI in order to characterize the extent of host cell infiltration and inflammatory cell accumulation within and near the transplanted formulations. DAPI staining (blue) revealed that many host cells surrounded the microcapsules and *in situ*-forming hydrogels, and ED1 staining (red) demonstrated macrophage accumulation at the surfaces and in tissues surrounding the microcapsules and *in situ*-forming hydrogels (Fig. 9A). Macrophages may act to remove the microcapsules and *in situ*-forming hydrogels from the injection site.[26] In addition, green fluorescence images showed that BSA-FITC remained inside the drug depot implants. The intensity and location of the fluorescent signal decreased with implantation time. The decreasing intensity of fluorescence in these experiments provides further evidence for the sustained release of BSA-FITC from drug depot implants.

ED1-positive cells were counted and normalized according to the total stained tissue area in order to determine the extent of inflammation (Fig. 9B). The CH-Cap drug depot implant exhibited slightly higher inflammation at 1 week. However, the number of ED1-positive cells in all formulations ranged from 15% to 25%, and the number of macrophages (ED1-positive cells) did not vary significantly between samples.

Conclusions

Important factors in the development of protein drug delivery systems are the stability of the loaded protein, encapsulation efficiency, and bioavailability of the released protein through lower initial burst release and longer duration of release. Through previous works, we achieved the preparation of protein-loaded microcapsules with stable loaded protein and high encapsulation efficiency. In this work, we focused on achieving a pronounced decrease in the protein initial burst release and a significantly extended duration of release from *in vivo* drug depot implants formed by protein-loaded

microcapsules and *in situ*-forming hydrogels through a minimally invasive manner. The drug depot implants sustained protein delivery for over the desired period, thus increasing the bioavailability of BSA through suppression in the initial burst release. We confirmed that the viscosity of the *in situ*-forming hydrogels was an important factor influencing release profiles. The injectable formulations in this work may provide numerous benefits as minimally invasive therapeutic drug depots and as useful experimental platforms for testing the sustained *in vivo* pharmacological performance of protein drugs. Thus, further research in large animal models using practical therapeutic protein-loaded microcapsules and the *in situ*-forming hydrogels investigated in this work is now in progress.

Acknowledgements

This study was supported by a grant from Pioneer Research Center Program (2010-0002170) and Priority Research Centers Program (2010-0028294) through NRF funded by the Ministry of Education, Science and Technology.

References

1 J. M. Davidson, *J. Invest. Dermatol.*, 2008, **128**, 1360–1362.
2 K. M. Dhirendra, S. Baboota, A. Ahuja, S. Hasan and J. Ali, *Curr. Drug Delivery*, 2007, **4**, 141–151.
3 M. Ye, S. Kim and K. Park, *J. Controlled Release*, 2010, **146**, 241–260.
4 R. M. Hernández, G. Orive, A. Murua and J. L. Pedraz, *Adv. Drug Delivery Rev.*, 2010, **62**, 711–730.
5 B. S. Kim, J. M. Oh, H. Hyun, K. S. Kim, S. H. Lee, Y. H. Kim, K. Park, H. B. Lee and M. S. Kim, *Mol. Pharmaceutics*, 2009, **6**, 353–365.
6 B. S. Kim, J. M. Oh, K. S. Kim, K. S. Seo, J. S. Cho, G. Khang, H. B. Lee, K. Park and M. S. Kim, *Biomaterials*, 2009, **30**, 902–909.
7 D. H. Choi, C. H. Park, I. H. Kim, H. J. Chun, K. Park and D. K. Han, *J. Controlled Release*, 2010, **147**, 193–201.
8 Y. Yeo and K. Park, *Arch. Pharmacal Res.*, 2004, **27**, 1–12.
9 C. Zheng and W. Liang, *Drug Delivery*, 2010, **17**, 77–82.
10 M. S. Kim, J. H. Kim, B. H. Min, H. J. Chun, D. K. Han and H. B. Lee, *Polym. Rev.*, 2011, **51**, 23–52.
11 M. S. Kim, S. J. Park, H. J. Chun and C. Kim, *Tissue Eng. Regener. Med.*, 2011, **8**, 117–123.
12 C. Tsitsilianis, *Soft Matter*, 2011, **7**, 2372–2388.
13 Y. Lu and M. Ballauff, *Prog. Polym. Sci.*, 2011, **36**, 767–792.
14 K. S. Kim, J. H. Lee, J. Y. Lee, B. Lee, H. B. Lee and M. S. Kim, *Biomaterials*, 2008, **29**, 4420–4428.
15 W. Zhang, Y. Shi, Y. Chen, J. Hao, X. Sha and X. Fang, *Biomaterials*, 2011, **32**, 5934–5944.
16 S. C. Park, S. H. Oh and J. H. Lee, *Tissue Eng. Regener. Med.*, 2011, **8**, 192–199.
17 M. D. Biase, P. Leonardis, V. Castelletto, I. W. Hamley, B. Derby and N. Tirelli, *Soft Matter*, 2011, **7**, 4928–4937.
18 Y. M. Kang, G. H. Kim, J. I. Kim, D. Y. Kim, B. N. Lee, S. M. Yoon, J. H. Kim and M. S. Kim, *Biomaterials*, 2011, **32**, 4556–4564.
19 J. I. Kim, S. H. Lee, H. J. Kang, D. Y. Kwon, D. Y. Kim, W. S. Kang, J. H. Kim and M. S. Kim, *Soft Matter*, 2011, **7**, 8650–8656.
20 J. Y. Lee, K. S. Kim, Y. M. Kang, E. S. Kim, S. J. Hwang, H. B. Lee, B. H. Min, J. H. Kim and M. S. Kim, *Int. J. Pharm.*, 2010, **392**, 51–56.
21 H. H. Ahn, K. S. Kim, J. H. Lee, J. Y. Lee, B. S. Kim, I. W. Lee, H. J. Chun, J. H. Kim, H. B. Lee and M. S. Kim, *Tissue Eng. A*, 2009, **15**, 1821–1832.
22 H. Hyun, Y. H. Kim, I. B. Song, J. W. Lee, M. S. Kim, G. Khang, K. Park and H. B. Lee, *Biomacromolecules*, 2007, **8**, 1093–1100.
23 A. Hatefia and B. Amsdena, *J. Controlled Release*, 2002, **80**, 9–28.
24 C. Chena, C. Fangb, S. A. Al-Suwayehc, Y. Leud and J. Fanga, *Int. J. Pharm.*, 2011, **415**, 119–128.
25 S. H. Lee, Y. Lee, S. W. Lee, H. Y. Ji, J. Lee, D. S. Lee and T. G. Park, *Acta Biomater.*, 2011, **7**, 1468–1476.
26 C. K. Colton, *Cell Transplant.*, 1995, **4**, 415–436.

Addition and correction

Note from RSC Publishing

This article was originally published with incorrect page numbers. This is the corrected, final version.

The Royal Society of Chemistry apologises for these errors and any consequent inconvenience to authors and readers.